Inorg. Chem. **2006**, *45*, 4850–4858

From a Trinuclear Platinum(III) Phosphido Derivative to a Platinum(II) Cluster: Formation of a P–C Bond†

Juan Forniés,* Consuelo Fortuño, Susana Ibáñez, and Antonio Martín

Departamento de Química Inorgánica and Instituto de Ciencia de Materiales de Aragón, Universidad de Zaragoza, CSIC, 50009 Zaragoza, Spain

Received February 16, 2006

Reaction of the trinuclear Pt^{III}–Pt^{III}–Pt^{II} $[(C_6F_5)_2Pt^{III}(\mu\text{-}PPh_2)_2Pt^{III}(\mu\text{-}PPh_2)_2Pt(C_6F_5)_2]$ (**2**) derivative with NBu_4Br or NBu_4I results in the formation of the trinuclear Pt^{II} complexes $[NBu_4][(PPh_2C_6F_5)(C_6F_5)Pt(\mu\text{-}PPh_2)(\mu\text{-}X)Pt(\mu\text{-}PPh_2)_2Pt(C_6F_5)_2]$ [X = I (**3**), Br (**4**)] through an intramolecular PPh_2/C_6F_5 reductive coupling and the formation of the phosphine $PPh_2C_6F_5$. The trinuclear Pt^{II} complex $[(PPh_2C_6F_5)(C_6F_5)Pt(\mu\text{-}PPh_2)Pt(\mu\text{-}PPh_2)_2Pt(C_6F_5)_2]$ (**5**), which displays two Pt–Pt bonds, can be obtained either by halide abstraction in **4** or by refluxing of **2** in CH_2Cl_2. This latter process also implies an intramolecular PPh_2/C_6F_5 reductive coupling. Treatment of complex **5** with several ligands (Br^-, H^-, and CO) results in the incorporation of the ligand to the cluster and elimination of one (X = H^-) or both (X = Br^-, CO) Pt–Pt bonds, forming the trinuclear complexes $[NBu_4][(PPh_2C_6F_5)(C_6F_5)Pt(\mu\text{-}PPh_2)(\mu\text{-}X)Pt(\mu\text{-}PPh_2)_2Pt(C_6F_5)_2]$ [X = Br (**6**), H (**7**)] or $[(PPh_2C_6F_5)(C_6F_5)Pt(\mu\text{-}PPh_2)_2Pt(\mu\text{-}PPh_2)(CO)Pt(C_6F_5)_2(CO)]$ (**8**). The structures of the complexes have been established on the basis of ^1H, ^{19}F, and ^{31}P NMR data, and the X-ray structures of the complexes **2**, **3**, **5**, and **7** have been established. The chemical relationship between the different complexes has also been studied.

Introduction

Pt^{III} is an unusual oxidation state. Only a few mononuclear complexes have been reported, and in some cases, they have been proposed as intermediates in the reductive elimination and oxidative addition reactions of Pt^{IV} and Pt^{II}, respectively.[1] Some unbridged dinuclear derivatives are known, but most of the dinuclear Pt^{III} complexes are doubly or quadruply bridged by bidentate ligands. In all these cases, the coordination environment of the Pt center is octahedral and the electron delocalization flexibility of the $Pt^{III}-Pt^{III}$ bond gives the Pt atoms both Pt^{II} and Pt^{IV} character.[1−5]

Recently, we have reported an unusual type of Pt_2^{III} complex that shows C donor ligands or diphenylphosphido groups as monodentate bridging ligands.[6−8] Surprisingly, in this last type of complex, the $Pt^{III}-Pt^{III}$ bond is contained in the metal coordination planes. Oxidation of a di- or trinuclear diphenylphosphido palladium or platinum(II) complex is not a simple process, and the results are strongly dependent on the starting material and on the oxidant used. Thus, the binuclear complex $[NBu_4]_2[(C_6F_5)_2Pt(\mu\text{-}PPh_2)_2Pt(C_6F_5)_2]$ reacts with Ag^+, yielding the stable binuclear $[(C_6F_5)_2Pt^{III}(\mu\text{-}PPh_2)_2Pt^{III}(C_6F_5)_2]$ $Pt^{III}-Pt^{III}$ compound, which displays a Pt−Pt bond (30 valence electron count),[8] while oxidation with I_2 forms the same $Pt^{III}-Pt^{III}$ compound, which, in the presence of the I^- formed, produces an intramolecular PPh_2/C_6F_5 reductive coupling and the formation of the binuclear $Pt^{II}-Pt^{II}$ $[NBu_4][(PPh_2C_6F_5)(C_6F_5)Pt(\mu\text{-}PPh_2)(\mu\text{-}I)Pt(C_6F_5)_2]$ compound (Scheme 1a).[9]

As far as the trinuclear complexes are concerned, oxidation of the Pt^{II} complex $[NBu_4]_2[(C_6F_5)_2Pt(\mu\text{-}PPh_2)_2Pt(\mu\text{-}PPh_2)_2$-

† Polynuclear Homo- or Heterometallic Palladium(II)−Platinum(II) Pentafluorophenyl Complexes Containing Bridging Diphenylphosphido Ligands. 22. For part 21, see ref 57.

* To whom correspondence should be addressed. E-mail: juan.fornies@unizar.es.

(1) Rendina, L. M.; Hambley, T. W. In *Comprehensive Coordination Chemistry II*; McCleverty, J. A., Meyer, T. J., Eds.; Elsevier Inc.: San Diego, 2004; Vol. 6.
(2) Matsumoto, K.; Ochiai, M. *Coord. Chem. Rev.* **2002**, *231*, 229−238.
(3) Lippert, B. *Coord. Chem. Rev.* **1999**, *182*, 263−295.
(4) Ochiai, M.; Lin, Y.-S.; Yamada, J.; Misawa, H.; Arai, S.; Matsumoto, K. *J. Am. Chem. Soc.* **2004**, *126*, 2536−2445.
(5) Iwatsuki, S.; Mizushima, C.; Morimoto, N.; Muranaka, S.; Ishihara, K.; Matsumoto, K. *Inorg. Chem.* **2005**, *44*, 8097−8104.
(6) Usón, R.; Forniés, J.; Tomás, M.; Casas, J. M.; Cotton, F. A.; Falvello, L. R.; Feng, X. *J. Am. Chem. Soc.* **1993**, *115*, 4145−4154.
(7) Usón, R.; Forniés, J.; Falvello, L. R.; Tomás, M.; Casas, J. M.; Martín, A.; Cotton, F. A. *J. Am. Chem. Soc.* **1994**, *116*, 7160−7165.
(8) Alonso, E.; Casas, J. M.; Cotton, F. A.; Feng, X. J.; Forniés, J.; Fortuño, C.; Tomás, M. *Inorg. Chem.* **1999**, *38*, 5034−5040.
(9) Chaouche, N.; Forniés, J.; Fortuño, C.; Kribii, A.; Martín, A.; Karipidis, P.; Tsipis, A. C.; Tsipis, C. A. *Organometallics* **2004**, *23*, 1797−1810.

10.1021/ic0602695 CCC: $33.50
Published on Web 05/05/2006

Scheme 1

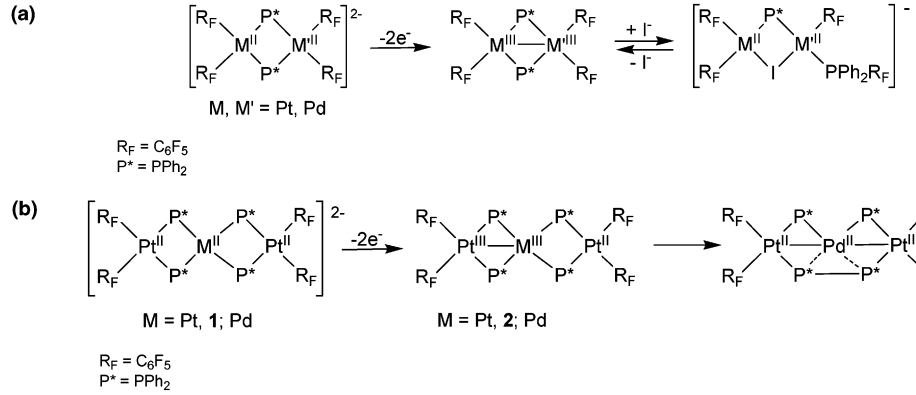

Scheme 2

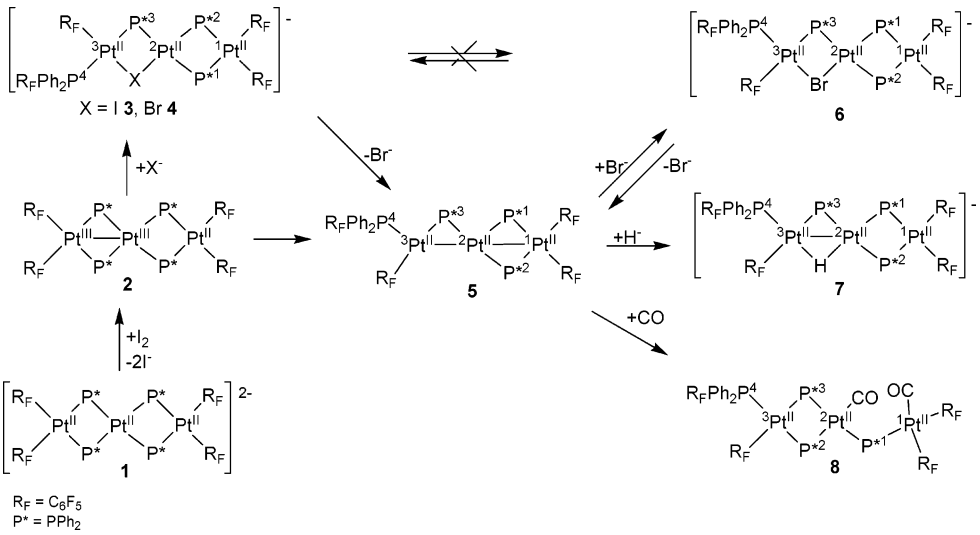

$Pt(C_6F_5)_2]$ (**1**) with Ag^+ produces $[(C_6F_5)_2Pt^{III}(\mu\text{-}PPh_2)_2Pt^{III}(\mu\text{-}PPh_2)_2Pt(C_6F_5)_2]$ (**2**), a cluster with a 46 valence electron count that displays a Pt−Pt bond coplanar to the plane of the metal skeleton (Scheme 1b).[10] Surprisingly, the reaction of the heterotrinuclear compound $[NBu_4]_2[(C_6F_5)_2Pt(\mu\text{-}PPh_2)_2\text{-}Pd(\mu\text{-}PPh_2)_2Pt(C_6F_5)_2]$ with Ag^+ does not produce the homologous $Pt^{III}-Pd^{III}-Pt^{II}$ derivative. In fact, although oxidation takes place, a very striking intramolecular reductive coupling of two PPh_2 groups forms tetraphenyldiphosphine, yielding the 44 skeleton valence electron count $[PdPt_2(\mu\text{-}PPh_2)_2(\mu\text{-}Ph_2P-PPh_2)(C_6F_5)_4]$ (Scheme 1b).[11]

The different behavior of Ag^+ or I_2 toward the binuclear phosphido complexes and the surprising results obtained when the trinuclear complexes are treated with Ag^+ prompted us to investigate the reaction of the trinuclear derivative **1** toward I_2 and the stability/reactivity of the resulting compound.

Results and Discussion

Synthesis. The reaction of a yellow suspension of **1** in 1,2-dichloroethane with I_2 (1:1 molar ratio), at room temperature, produces a red solution from which **2** is isolated in 73% yield. When the reaction is carried out at reflux temperature for 2 h, a yellow solution is obtained from which the trinuclear Pt^{II} complex $[NBu_4][(PPh_2C_6F_5)(C_6F_5)Pt(\mu\text{-}PPh_2)(\mu\text{-I})Pt(\mu\text{-}PPh_2)_2Pt(C_6F_5)_2]$ (**3**) crystallizes (Scheme 2). As was previously commented on, the formation of complex **2** can also be achieved by reacting complex **1** with Ag^+, and in this process, no evolution of **2** is observed. This means that the presence of the I^- formed in the reaction system forces a PPh_2/C_6F_5 reductive coupling and the formation of **3**. Similarly, the bromo derivative $[NBu_4][(PPh_2C_6F_5)(C_6F_5)\text{-}Pt(\mu\text{-}PPh_2)(\mu\text{-Br})Pt(\mu\text{-}PPh_2)_2Pt(C_6F_5)_2]$ (**4**), analogous to **3**, is obtained through the reaction of the Pt^{III} derivative **2** with NBu_4Br. The treatment of **4** with $AgClO_4$ in CH_2Cl_2 results in the precipitation of AgBr and the isolation of $[(PPh_2C_6F_5)\text{-}(C_6F_5)Pt(\mu\text{-}PPh_2)Pt(\mu\text{-}PPh_2)_2Pt(C_6F_5)_2]$ (**5**; Scheme 2) as a orange solid.

Elimination of the bridging bromo ligand means, in fact, the elimination of 4 electrons of the molecular skeleton, giving an unsaturated species of 44 electrons, which requires, if no further rearrangement of the ligands occurs, the formation of two M−M bonds.[12−15] The formation of

(10) Alonso, E.; Casas, J. M.; Forniés, J.; Fortuño, C.; Martín, A.; Orpen, A. G.; Tsipis, C. A.; Tsipis, A. C. *Organometallics* **2001**, *20*, 5571−5582.

(11) Forniés, J.; Fortuño, C.; Ibáñez, S.; Martín, A.; Tsipis, A. C.; Tsipis, C. A. *Angew. Chem., Int. Ed.* **2005**, *44*, 2407−2410.

(12) Forniés, J.; Fortuño, C.; Gil, R.; Martín, A. *Inorg. Chem.* **2005**, *44*, 9534−9541.

(13) Alonso, E.; Forniés, J.; Fortuño, C.; Martín, A.; Orpen, A. G. *Chem. Commun.* **1996**, 231−232.

complex **5** from **4** is a somewhat different process from that occurring when I is eliminated from the binuclear $[(PPh_2C_6F_5)(C_6F_5)Pt^{II}(\mu\text{-}PPh_2)(\mu\text{-}I)Pt^{II}(C_6F_5)_2]^-$, which gives $[(C_6F_5)_2Pt^{III}(\mu\text{-}PPh_2)_2Pt^{III}(C_6F_5)_2]$ (Scheme 1a).[9] In this latter case, the elimination of the bridging iodo ligand (four-electron donor) of the binuclear Pt^{II} complex would give a much more unsaturated intermediate "$(PPh_2C_6F_5)(C_6F_5)Pt^{II}(\mu\text{-}PPh_2)Pt^{II}(C_6F_5)_2$", which would require the formation of a Pt−Pt double bond. However, this does not occur in the case in hand, but rather there is a saturation of the skeleton through a very rare[16−18] intramolecular oxidative addition of $PPh_2C_6F_5$ and the formation of the $Pt^{III}-Pt^{III}$ compound with a Pt−Pt bond.[9]

Complexes **2** and **5** are constitutional isomers (Scheme 2), and the synthesis of **5** prompted us to investigate if complex **2** is, in fact, an intermediate of **5**. When a red solution of **2** in 1,2-dichloroethane is refluxed for 40 h, the solution turns yellow and **5** crystallizes from the concentrated solution (Scheme 2). This transformation is remarkable because it implies a reductive coupling of PPh_2 and C_6F_5 to form the phosphine, $PPh_2C_6F_5$. It also contrasts with the spontaneous formation of the tetraphenyldiphosphine compound $[PdPt_2(\mu\text{-}PPh_2)_2(\mu\text{-}Ph_2P-PPh_2)(C_6F_5)_4]$ when the homologous $Pt^{II}-Pd^{II}-Pt^{II}$ is oxidized with Ag^+ because this process implies a PPh_2/PPh_2 reductive coupling (Scheme 1b).

It is well-known that tertiary phosphines can be converted thermally to phosphido bridges as a result of P−C bond activation and the formation of new M−P and M−C bonds.[17−26] The reverse process is less frequent,[27,28] and in some cases [P−C(phenyl),[29] P−C(perfluorophenyl),[9] and P−C(alkynyl)[30]], the process is even reversible. The synthesis of **3**−**5** from **2** confirms that the phosphido Pt^{III} complexes favor the coupling of pentafluorophenyl and phosphide ligands to afford Pt^{II} derivatives.

(14) Alonso, E.; Forniés, J.; Fortuño, C.; Martín, A.; Orpen, A. G. *Organometallics* **2001**, *20*, 850−859.
(15) Falvello, L. R.; Forniés, J.; Fortuño, C.; Durán, F.; Martín, A. *Organometallics* **2002**, *21*, 2226−2234.
(16) Heyn, R. H.; Gorbitz, C. H. *Organometallics* **2002**, *21*, 2781−2784.
(17) Ang, H. G.; Kwik, W. L.; Leong, W. K.; Johnson, B. F. G.; Lewis, J.; Raithby, P. R. *J. Organomet. Chem.* **1990**, *396*, C43.
(18) Fahey, D. R.; Mahan, J. E. *J. Am. Chem. Soc.* **1976**, *98*, 4499−4503.
(19) García, G.; García, M. E.; Melón, S.; Riera, V.; Ruiz, M. A.; Villafañe, F. *Organometallics* **1997**, *16*, 624−631.
(20) Shiu, K. B.; Jean, S. W.; Wang, S. L.; Liao, F. L.; Wang, J. C.; Liou, L. S. *Organometallics* **1997**, *16*, 114−119.
(21) Dubois, R. A.; Garrou, P. E. *Organometallics* **1986**, *5*, 460−466.
(22) Bender, R.; Braunstein, P.; Dedieu, A.; Ellis, P. D.; Huggins, B.; Harvey, P. D.; Sappa, E.; Tiripicchio, A. *Inorg. Chem.* **1996**, *35*, 1223−1234.
(23) Mizuta, T.; Onishi, M.; Nakazono, T.; Nakazawa, H.; Miyoshi, K. *Organometallics* **2002**, *21*, 717−726.
(24) Geoffroy, G. L.; Rosenberg, S.; Shulman, P. M.; Whittle, R. R. *J. Am. Chem. Soc.* **1984**, *106*, 1519−1521.
(25) Shulman, P. M.; Burkhardt, E. D.; Lundquist, E.; Pilato, R. S.; Geoffroy, G. L.; Rheingold, A. L. *Organometallics* **1987**, *6*, 101−109.
(26) Zhuravel, M. A.; Moncarz, J. R.; Glueck, D. S.; Lam, K.-C.; Rheingold, A. L. *Organometallics* **2000**, *19*, 3447−3454.
(27) Archambault, C.; Bender, R.; Braunstein, P.; Decian, A.; Fischer, J. *Chem. Commun.* **1996**, 2729−2730.
(28) Falvello, L. R.; Forniés, J.; Fortuño, C.; Martín, A.; Martínez-Sariñena, A. P. *Organometallics* **1997**, *16*, 5849−5856.
(29) Cabeza, J. A.; del Río, I.; Riera, V.; García-Granda, S.; Sanni, B. *Organometallics* **1997**, *16*, 1743−1748.
(30) Albinati, A.; Filippi, V.; Leoni, P.; Marchetti, L.; Pasquali, M.; Passarelli, V. *Chem. Commun.* **2005**, 2155−2157.

Table 1. $^{31}P\{^1H\}$ NMR Data for **3**−**8** (*J* in Hz)

	complex					
	3[a]	**4**[a]	**5**[b]	**6**[a]	**7**[b]	**8**[c]
δP(1)	−151.7	−142.6	251.8	−127.8	−124.5	−6.6
δP(2)	−135.1	−126.1	281.2	−143.2	−140.7	−121.1
δP(3)	−44.3	−25.2	132.6	−35.4	94.3	−136.2
δP(4)	14.7	19.3	20.7	−0.5	13.8	8.0
J[P(1)−P(2)]	156	167	89	163	128	
J[P(1)−P(3)]	284	286		195		
J[P(1)−P(4)]			80		48	
J[P(2)−P(3)]			116	276	241	155
J[P(2)−P(4)]			56			351
J[P(3)−P(4)]	321	321				
^1J[Pt−P(1)]	1762	ca. 1700	1964	2986	2626	1689
	1625	*d*	1392	1988	1907	1489
^2J[Pt(3)−P(1)]			190			
^1J[Pt−P(2)]	2778	2810	2216	ca. 1800	ca. 1700	2397
	1972	1994	1032	d	*d*	1952
^2J[Pt(3)−P(2)]			84			
^1J[Pt−P(3)]	1822	1912	2830	ca. 1580	ca. 1750	1733
	1640	1690	2263	d	*d*	1071
^1J[Pt(3)−P(4)]	2239	2260	4368	4861	4140	2211
^2J[Pt(2)−P(4)]			482		51	
^2J[Pt(1)−P(3)]			116			

[a] In deuterioacetone. [b] In CD_2Cl_2. [c] In $CDCl_3$. [d] The Pt satellites appear overlapped, and the two ^1J(Pt−P) values cannot be accurately measured.

Complex **5** adds bromide easily, giving rise to a 48-electron saturated complex $[(PPh_2C_6F_5)(C_6F_5)Pt(\mu\text{-}PPh_2)(\mu\text{-}Br)Pt(\mu\text{-}PPh_2)_2Pt(C_6F_5)_2]^-$ (**6**), an isomer of **4**, in which the $PPh_2C_6F_5$ ligand is coordinated in a cis disposition to the phosphido ligand (Scheme 2). As expected, the elimination of the bromo ligand from **6** as AgBr forms **5** again. All structural data for complex **6** are given in the Experimental Section and in Table 1. We have not detected the transformation of complex **4** into its isomer **6** or vice versa when acetone solutions of the respective complexes are kept at room temperature for 2 months.

The reaction of complex **5** with $[NBu_4][BH_4]$ yields the hydrido derivative $[NBu_4][(PPh_2C_6F_5)(C_6F_5)Pt(\mu\text{-}PPh_2)(\mu\text{-}H)Pt(\mu\text{-}PPh_2)_2Pt(C_6F_5)_2]$ (**7**; Scheme 2), a complex with a total valence electron count of 46 that requires the presence of a Pt−Pt bond, as can be seen in the X-ray diffraction structure. Considering that the cluster **5** and the heterotrinuclear $[PdPt_2(\mu\text{-}PPh_2)_2(\mu\text{-}Ph_2P-PPh_2)(C_6F_5)_4]$ (see Scheme 1b) are the result of the evolution of the same type of intermediate, $[(C_6F_5)_2Pt^{III}(\mu\text{-}PPh_2)_2M^{III}(\mu\text{-}PPh_2)_2Pt(C_6F_5)_2]$ (M = Pt, Pd), the different reactivities of both complexes with NBu_4BH_4 are noteworthy. The heterotrinuclear complex adds 2 electrons and produces the transformation of the diphosphine bridging ligand into two bridging phosphido ligands, yielding $[NBu_4]_2[(C_6F_5)_2Pt(\mu\text{-}PPh_2)_2Pd(\mu\text{-}PPh_2)_2Pt(C_6F_5)_2]$,[11] while the addition of 2 electrons to the Pt^{II} cluster **5** along with the oxidative addition of the $Ph_2P-C_6F_5$ bond to give the Pt^{II} **1** seems to be an unfavorable process, and the hydride derivative **7** is obtained instead.

The behavior of cluster **5** toward CO is different from its behavior toward the bromo or hydrido ligands, although the three ligands can act as terminal or bridging ligands. A CH_2Cl_2 solution of cluster **5** reacts with CO, yielding the saturated dicarbonyl 48-electron complex $[(PPh_2C_6F_5)(C_6F_5)Pt(\mu\text{-}PPh_2)_2Pt(\mu\text{-}PPh_2)(CO)Pt(C_6F_5)_2(CO)]$ (**8**). All attempts to obtain a suitable crystal for X-ray study have been unsuc-

Scheme 3

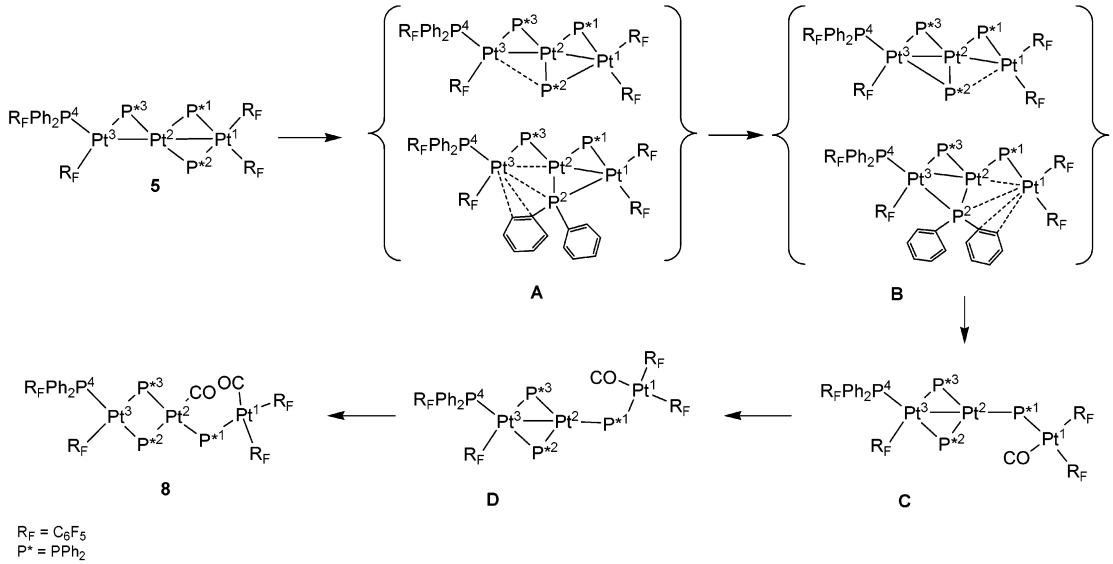

cessful, and the structure of complex **8** can only be assigned tentatively as depicted in Scheme 2. The synthesis of complex **8** from **5** implies the cleavage of the Pt(1)−P(2) bond and the formation of the Pt(3)−P(2) bond, i.e., the migration of the P(2)Ph_2 group. A plausible mechanism for the formation of **8** is depicted in Scheme 3 and could imply the formation of intermediates (**A** and **B**) in which the P(2)-Ph_2 group is bridging the three metal centers with or without η^2-phenyl−Pt interaction. Such a μ^3-bonding mode for the μ-PR_2 ligand is not very frequent, although some examples have been reported.[31−37] In addition, this coordination mode has been proposed as an intermediate for phosphido migration processes.[15] The addition of CO to **B** decreases the unsaturation, yielding a 46-electron compound **C** with a Pt−Pt bond and in which all of the phosphido groups act as bridging ligands between the two metal centers. This intermediate **C** is closely related to the reported 30-electron dinuclear complex $[(C_6F_5)_2Pt(\mu\text{-}PPh_2)_2Pt(PPh_3)]$[38] that shows an unsaturated Pt center, which easily adds a two-electron terminal ligand. The addition of a CO ligand to the unsaturated Pt(2) in **C** would easily yield complex **8**. Cluster **5** does not react with PPh_3 (1:1 molar ratio) or NCMe in excess. The bulkiness of the PPh_3 group could hinder its coordination to Pt(3) in **5** or to Pt(1) in **B**, and this may be why the reaction does not take place. However, we cannot provide a satisfactory explanation of why acetonitrile does not react with complex **5**.

Spectroscopic Properties. The ^{1}H NMR spectra of **3** and **4** have been recorded in deuterioacetone and show signals due the phenyl H atoms and the NBu_4^+ cation. The ^{19}F NMR provides conclusive evidence of the bonding of the pentafluorophenyl group either to a metal center or to a P atom.[9,28,39] The signals of the *o*-F of $PPh_2C_6F_5$ appear at higher field than those of the M−C_6F_5 system, while the *m*- and *p*-F ones appear at a lower field with respect to the pentafluorophenyl group bonded to M. The ^{19}F NMR spectra of **3** and **4** (deuterioacetone solution; see the Experimental Section) show, in the *o*-F region, four signals of similar intensity: three of them with Pt satellites due to the three pentafluorophenyl ligands and another one assigned to $PPh_2C_6F_5$, in full agreement with the inequivalence of the four C_6F_5 groups. At a higher field (*m*- and *p*-F regions), two signals (1:2 intensity ratio) due to the *p*- and *m*-F atoms of $PPh_2C_6F_5$ and four overlapped signals (3:4:1:1 intensity ratio) due to the three M−C_6F_5 groups are observed. The ^{31}P{^{1}H} NMR spectra of both **3** and **4** in deuterioacetone display the same pattern (see Table 1). The δP values of the phosphido ligands are highly informative, and the spectra are conclusive for the structural assignment of the two complexes. The signals due to the P(1) (doublet of doublets) and P(2) (doublet) atoms (see Scheme 2 for atom numbering) appear from −126.1 to −151.7 ppm, in the range observed for complexes in which two PPh_2 groups are bonded to two metal centers without a M−M bond.[14,15,38,40−42] The P(3) atom appears as a doublet of doublets at −44.3 (**3**) and −25.2 (**4**) ppm, in the range expected for a "Pt(μ-PPh_2)(μ-X)Pt" (X = Cl, Br, I, OH)[9,39,41,43,44] fragment with a long Pt···Pt distance [3.477(1) Å for **3** in the solid]. The signal due to

(31) Englich, U.; Hassler, K.; Ruhlandt-Senge, K.; Unlig, F. *Inorg. Chem.* **1998**, *37*, 3532−3537.
(32) Eichhofer, A.; Fenske, D.; Holstein, W. *Angew. Chem., Int. Ed. Engl.* **1993**, *32*, 242−245.
(33) Bender, R.; Braunstein, P.; Dedieu, A.; Dusausoy, Y. *Angew. Chem., Int. Ed. Engl.* **1989**, *28*, 923−925.
(34) Corrigan, J. F.; Doherty, S.; Taylor, N. J. *J. Am. Chem. Soc.* **1992**, *114*, 7557−7558.
(35) Pechmann, T.; Brandt, C. D.; Werner, H. *Dalton Trans.* **2004**, 959−966.
(36) Leca, F.; Sauthier, M.; Deborde, V.; Toupet, L.; Réau, R. *Chem.−Eur. J.* **2003**, *9*, 3785−3795.
(37) Braunstein, P.; Boag, N. M. *Angew. Chem., Int. Ed.* **2001**, *40*, 2427−2433.
(38) Falvello, L. R.; Forniés, J.; Fortuño, C.; Martínez, F. *Inorg. Chem.* **1994**, *33*, 6242−6246.
(39) Ara, I.; Chaouche, N.; Forniés, J.; Fortuño, C.; Kribii, A.; Tsipis, A. C. *Organometallics* **2006**, *25*, 1084−1091.
(40) Alonso, E.; Forniés, J.; Fortuño, C.; Martín, A.; Orpen, A. G. *Organometallics* **2003**, *22*, 5011−5019.
(41) Alonso, E.; Forniés, J.; Fortuño, C.; Tomás, M. *J. Chem. Soc., Dalton Trans.* **1995**, 3777−3784.
(42) Forniés, J.; Fortuño, C.; Navarro, R.; Martínez, F.; Welch, A. J. *J. Organomet. Chem.* **1990**, *394*, 643−658.
(43) Ara, I.; Chaouche, N.; Forniés, J.; Fortuño, C.; Kribii, A.; Tsipis, A. C.; Tsipis, C. A. *Inorg. Chim. Acta* **2005**, *358*, 1377−1385.

the $PPh_2C_6F_5$ ligand appears as a doublet, 321 Hz in both complexes, in the range expected for this ligand. This large ^2J[P(3)−P(4)] value is in accordance with the trans disposition of the $PPh_2C_6F_5$ ligand and the P(3)Ph_2 group. All signals show Pt satellites, and for the P atoms of phosphido ligands, two values of ^1J(Pt−P) can be measured. For the signal due to P(2), these two values can tentatively be assigned. The coupling constants of P(1) with Pt(1) and with Pt(2) are similar (ca. 1700 Hz), and the same holds true for the coupling of P(3) with Pt(2) and with Pt(3). Nevertheless, the two ^1J[Pt−P(2)] values are different, ca. 2000 and 2800 Hz. Taking into account that the Pt(1)−P(1) and Pt(1)−P(2) bonds are in trans disposition to the C_6F_5 groups, the ^1J[Pt(1)−P(1)] and ^1J[Pt(1)−P(2)] values may be similar. Thus, the lowest value of ^1J[Pt−P(2)] (ca. 2000 Hz) can be assigned to ^1J[Pt(1)−P(2)] and the 2800-Hz value to ^1J[Pt(2)−P(2)]. This assignment is in agreement with the higher trans influence of the C_6F_5 group with respect to the halo ligands.

Although the IR spectra of **3** and **4** do not provide any important structural information, they unambiguously indicate the presence of the $PPh_2C_6F_5$ ligand. Besides the strong signals around 1500 and 950 cm^{-1} always observed in all pentafluorophenyl derivatives with a M−C_6F_5 bond,[45,46] two other absorptions at higher frequencies, ca. 1520 and 980 cm^{-1}, assignable to the $PPh_2C_6F_5$ ligand[9,28,39] are observed.

The ^{19}F NMR spectrum of **5** in CD_2Cl_2 shows, in the *o*-F region, four signals of the same intensity, three of them with Pt satellites, as in **3** and **4**. Several overlapped signals appear in the *m*- and *p*-F atom region (see the Experimental Section). The ^{31}P{^{1}H} NMR spectrum of **5** shows four signals with Pt satellites (see Table 1). The chemical shift of P(4) (see Scheme 2 for atom numbering) is analogous to those observed for **3** and **4**, but the δP values of the three phosphido bridging ligands appear at a lower field. The signals due to P(1) and P(2) appear at 251.8 and 281.2 ppm, respectively, in the region expected for a "Pt(μ-PPh_2)$_2$Pt" fragment with a M−M bond.[8,10,28,38,47,48] The P(3) signal appears at a higher field than P(1) and P(2) signals, 132.6 ppm, and within the range found in all of our compounds containing a single phosphido ligand bridging two metal centers with a M−M bond.[14,48] It is noteworthy that a value of ^2J(Pt−P) can be measured for each signal from their Pt satellites in addition to ^1J(Pt−P) couplings. These ^2J(Pt−P) couplings have been observed in our unsaturated complexes with short intermetallic distances, for which M−M bonds have been proposed ("*Pt*(μ-PPh_2)$_2$M−*P*"[28,38,48] and "*Pt*(μ-PPh_2)M−*P*"[14,15,48]), while these Pt−P couplings are not observed for saturated complexes with long Pt···M distances. All data point to the presence of two M−M bonds in this 44-electron trinuclear compound **5**. The presence of the Pt(1)−Pt(2) bond is also supported by the δP values of P(1) and P(2) and the value of 116 Hz observed for ^2J[Pt(1)−P(3)]. The δP value of P(3), the values of ^2J[Pt(2)−P(4)] (482 Hz), ^2J[Pt(3)−P(1)] (190 Hz), and ^2J[Pt(3)−P(2)] (84 Hz), and the coupling through three bonds of P(1) and P(2) with P(4) (80 and 56 Hz, respectively) support the presence of the Pt(2)−Pt(3) bond. ^3J[P(1)−P(4)] is greater than ^3J[P(2)−P(4)] as a consequence of the fact that the P(4)−Pt−Pt−P(1) arrangement is more linear than P(4)−Pt−Pt−P(2) (see the X-ray structure).

The IR spectrum of **7** does not allow the detection of any absorption due to the Pt−(μ-H)−Pt system, although it is well-known that such absorptions (ca. 1600 cm^{-1}) are usually weak and often difficult to assign.[12,14,49,50] The ^{1}H NMR spectra of **7** in CD_2Cl_2 show signals due the phenyl H atoms and the NBu_4^+ cation with the expected intensity ratio, along with a signal centered at −4.7 ppm assignable to the bridging hydride. This signal appears as a doublet of doublets of triplets (104, 40, and 9 Hz), which is transformed into a doublet of triplets (40 and 9 Hz) in the ^{1}H {^{31}P} NMR experiment with irradiation in the P(4) resonance region (see Scheme 2 for atom numbering). These three couplings can be assigned unequivocally to ^1J[P(4)−H], ^1J[P(1)−H], and ^1J[P(2)−H] = ^1J[P(3)−H], respectively. Two values of ^1J(Pt−H), 484 and 604 Hz, can be extracted from the Pt satellites, in agreement with the bridging nature of the hydrido group.[12,14,50−53] The ^{19}F NMR spectrum is analogous to those of **3**−**6** (see the Experimental Section). The most noteworthy feature of the ^{31}P{^{1}H} NMR spectrum of **7** is the low-field shift of the P(3) signal (94.3 ppm) when compared with that of **6** (−35.4 ppm). Such displacements toward lower fields are always characteristic of complexes containing both μ-phosphido and μ-hydrido ligands[12,14,26] and are in agreement with the presence of a Pt(3)−Pt(2) bond. The signal due to P(4) appears as a doublet in **7** due to the coupling with P(1) {^3J[P(4)−P(1)] = 48 Hz}, while in the bromo derivative **6**, the P(4)−P(1) coupling is not observed because it should be expected for a ^4J[P(4)−P(1)] value. In addition, this signal shows Pt satellites due to the coupling with Pt(3) {^1J[Pt(3)−P(4)] = 4140 Hz} as well as with Pt(2) {^2J[Pt(2)−P(4)] = 51 Hz}, while this coupling between the Pt(2) and P(4) atoms is not observed in the saturated complex **6**. Taking into account that the three-center two-electron interaction (3c-2e) in a "PtHPt" fragment can also be described as a protonated M−M bond,[26,54] the NMR data of **7** must be compared with those extracted for **5**. In complex **5**, the couplings of P(4) with P(1) and with P(2) through the Pt(2)−Pt(3) bond [the Pt(2)−Pt(3) distance is 2.741(1) Å] are 80 and 56 Hz, respectively, while in the hydride derivative **7**, the coupling of P(4) with P(1) through the Pt-

(44) Alonso, E.; Forniés, J.; Fortuño, C.; Martín, A.; Rosair, G. M.; Welch, A. J. *Inorg. Chem.* **1997**, *36*, 4426−4431.
(45) Maslowsky, E. J. *Vibrational Spectra of Organometallic Compounds*; Wiley: New York, 1997.
(46) Usón, R.; Forniés, J. *Adv. Organomet. Chem.* **1988**, *28*, 219−297.
(47) Alonso, E.; Forniés, J.; Fortuño, C.; Martín, A.; Orpen, A. G. *Organometallics* **2003**, *22*, 2723−2728.
(48) Alonso, E.; Forniés, J.; Fortuño, C.; Martín, A.; Orpen, A. G. *Organometallics* **2000**, *19*, 2690−2697.
(49) Ara, I.; Falvello, L. R.; Forniés, J.; Lalinde, E.; Martín, A.; Martínez, F.; Moreno, M. T. *Organometallics* **1997**, *16*, 5392−5405.
(50) Leoni, P.; Manetti, S.; Pasquali, M. *Inorg. Chem.* **1995**, *34*, 749.
(51) Itazaki, M.; Yasushi, N.; Osakada, K. *Organometallics* **2004**, *23*, 1610−1621.
(52) Hughes, R. P.; Ward, A. J.; Golen, J. A.; Incarvito, C. D.; Rheingold, A. L.; Zakharov, L. N. *Dalton Trans.* **2004**, 2720−2727.
(53) Venanzi, L. M. *Coord. Chem. Rev.* **1982**, *43*, 251.
(54) van Leeuwen, P. W. N. M.; Roobeek, C. F.; Frijns, J. H. G.; Orpen, A. G. *Organometallics* **1990**, *9*, 1211−1222.

Table 2. Crystal Data and Structure Refinement for Complexes **3**·1.4Me_2CO, **5**·CH_2Cl_2, and **7**

	3·1.4Me_2CO	**5**·CH_2Cl_2	**7**
empirical formula	$C_{88}H_{76}F_{20}INP_4Pt_3$·1.4$Me_2CO$	$C_{72}H_{40}F_{20}P_4Pt_3$·$CH_2Cl_2$	$C_{88}H_{77}F_{20}NP_4Pt_3$
fw	2444.86	2079.12	2237.66
cryst size (mm)	0.41 × 0.21 × 0.11	0.48 × 0.35 × 0.22	0.40 × 0.29 × 0.19
temp (K)	100(1)	100(1)	100(1)
cryst syst	triclinic	monoclinic	monoclinic
space group	$P-1$	$P2_1/c$	$P2_1$
a (Å)	12.146(3)	20.222(2)	12.153(3)
b (Å)	17.504(4)	29.667(3)	28.295(7)
c (Å)	23.088(6)	23.584(2)	13.516(4)
α (deg)	102.013(5)	90	90
β (deg)	96.383(5)	103.835(3)	115.801(4)
γ (deg)	106.136(4)	90	90
V (Å^3), Z	4536.7(18)	8752.35(9)	4184.3(18), 4
Z	2	8	2
d_c (g cm^{-3})	1.790	2.011	1.776
μ (mm^{-1})	5.113	6.365	5.169
θ range (deg)	1.73−25.03	1.38−25.03	1.44−26.06
no. of reflns collected	24908	72209	23032
no. of unique reflns	15801, R_{int} = 0.0327	24151, R_{int} = 0.0555	12874, R_{int} = 0.0496
final R indices [$I > 2\sigma(I)$][a]	R1 = 0.0594, wR2 = 0.1410	R1 = 0.0291, wR2 = 0.0495	R1 = 0.0455, wR2 = 0.1012
R indices (all data)	R1 = 0.0694, wR2 = 0.1459	R1 = 0.0390, wR2 = 0.0509	R1 = 0.0535, wR2 = 0.1045
GOF[b] on F^2	1.153	0.981	1.012

[a] $wR2 = [\sum w(F_o^2 - F_c^2)^2/\sum wF_o^4]^{0.5}$; $R1 = \sum||F_o| - |F_c||/\sum|F_o|$. [b] Goodnes of fit $= [\sum w(F_o^2 - F_c^2)^2/(N_{obs} - N_{param})]^{0.5}$.

(2)−Pt(3) bond [the Pt(2)−Pt(3) distance is 2.848(1) Å] is smaller, 48 Hz, and the P(4)−P(2) coupling is not observed. In this context, in complex **5**, the couplings between Pt(2) and P(4), Pt(3) and P(1), and Pt(3) and P(2) (482, 190, and 84 Hz, respectively) are observed, while in **7**, these couplings, through the protonated Pt(2)−Pt(3) bond, must be smaller and only the ^2J[Pt(2)−P(4)] value, 51 Hz, can be extracted from the spectrum.

The ^{19}F NMR spectrum of **8** (see the Experimental Section) is similar to those observed for complexes **3**−**7**, and it indicates that the four C_6F_5 groups are inequivalent in solution at room temperature; i.e., the disposition of the C_6F_5 groups in **8** can be assumed to be the same as that in the starting material. The $^{31}P\{^1H\}$ NMR spectrum is conclusive to establish the relative disposition of the phosphido groups in this trinuclear complex, and it unambiguously indicates that, unlike the starting material **5**, the Pt(2) and Pt(3) atoms are joined by two phosphido groups while the Pt(1) and Pt(2) atoms are joined by a single PPh_2 ligand, as is depicted in Scheme 2. All data extracted from the spectrum are shown in Table 1. The chemical shift of the P(1) atom appears at lower field than those observed for P(2) and P(3), in agreement with the presence of the "Pt(μ-PPh_2)Pt" and "Pt(μ-PPh_2)$_2$Pt" fragments, respectively, without a M−M bond. These assignments are carried out easily from the coupling between the P atoms. The P(4) atom is coupled only with the P(2) atom, and the P(1) atom is coupled only with the P(3) atom. It has to be noted that the coupling between the P atoms of two phosphido ligands bonded to a Pt center in a cis disposition is usually observed only for the "Pt(μ-PPh_2)$_2$Pt" fragments. The coupling between P(2) and P(3) in **8** is 155 Hz, which indicates that these two PPh_2 ligands are involved in a "Pt(μ-PPh_2)$_2$Pt" fragment.

X-ray Diffraction Studies. The crystal structures of **3**, **5**, and **7** have been determined by an X-ray diffraction study. Crystal data and refinement parameters are given in Table 2. The structure of the complex ion of **3** together with the atom-labeling scheme is shown in Figure 1. Selected bond distances and angles are listed in Table 3. **3** is a trinuclear complex in which the Pt atoms lie at the center of square-planar environments. The three metal centers form almost a linear array [Pt(1)−Pt(2)−Pt(3) = 158.1(1)°], with long intermetallic distances [Pt(1)···Pt(2) = 3.600(1) Å; Pt(2)···Pt(3) = 3.477(1) Å], excluding the presence of M−M bonds. Pt(1) and Pt(2) are bridged by two diphenylphosphide ligands, while Pt(2) and Pt(3) are held together by a diphenylphosphide and a iodo bridge. The presence of $PPh_2C_6F_5$ in **3** is noteworthy. The P−C bond of this ligand is formed by coupling of the diphenylphosphido and pentafluorophenyl groups. The environments of Pt(1) and Pt(2) are coplanar, and these atoms and all others attached to them essentially lie in the same plane. The dihedral angle of this plane and the square plane of Pt(3) is 51.4°. This is most likely caused by the very different size of the bridging donor atom (I or P), as was previously observed in complexes [(PPh_3)(C_6F_5)Pt(μ-PPh_2)(μ-I)Pt(μ-PPh_2)(μ-I)Pt(C_6F_5)(PPh_3)][43] and [($PPh_2C_6F_5$)(C_6F_5)Pd(μ-PPh_2)(μ-I)Pd(C_6F_5)$_2$]$^-$.[9]

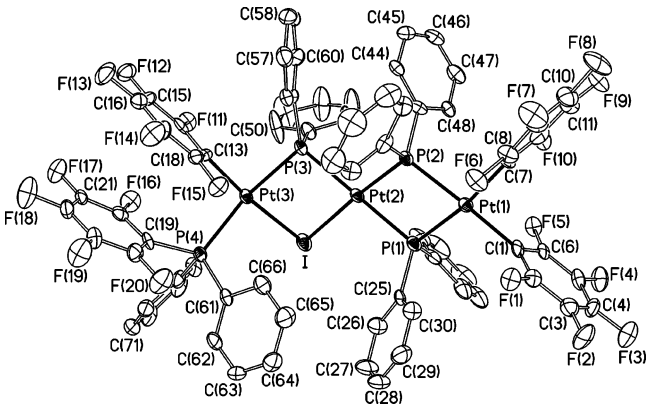

Figure 1. Molecular structure of the anion of complex **3**·1.4Me_2CO. Ellipsoids are drawn at their 50% probability level.

A drawing of the molecule of **5** together with the atom-labeling scheme is shown in Figure 2. Selected bond

Table 3. Selected Bond Lengths (Å) and Angles (deg) for **3**·1.4Me_2CO

Pt(1)−C(1)	2.052(10)	Pt(1)−C(7)	2.069(9)	Pt(1)−P(2)	2.289(3)
Pt(1)−P(1)	2.305(3)	Pt(2)−P(2)	2.268(2)	Pt(2)−P(1)	2.325(3)
Pt(2)−P(3)	2.347(3)	Pt(2)−I	2.7139(9)	Pt(3)−C(13)	2.019(9)
Pt(3)−P(3)	2.311(3)	Pt(3)−P(4)	2.318(3)	Pt(3)−I	2.6704(9)
Pt(1)···Pt(2)	3.600(1)	Pt(2)···Pt(3)	3.477(1)		
C(1)−Pt(1)−C(7)	88.6(4)	P(3)−Pt(3)−I	80.02(7)	P(2)−Pt(2)−I	176.15(7)
C(7)−Pt(1)−P(2)	95.0(3)	Pt(3)−I−Pt(2)	80.45(3)	P(3)−Pt(2)−I	78.49(7)
C(7)−Pt(1)−P(1)	171.8(3)	Pt(2)−P(2)−Pt(1)	104.38(10)	C(13)−Pt(3)−P(4)	91.9(3)
P(2)−Pt(2)−P(1)	76.75(9)	C(1)−Pt(1)−P(2)	175.9(3)	C(13)−Pt(3)−I	174.0(3)
P(1)−Pt(2)−P(3)	176.01(9)	C(1)−Pt(1)−P(1)	99.6(3)	P(4)−Pt(3)−I	93.85(7)
P(1)−Pt(2)−I	99.72(7)	P(2)−Pt(1)−P(1)	76.74(9)	Pt(1)−P(1)−Pt(2)	102.06(10)
C(13)−Pt(3)−P(3)	94.0(3)	P(2)−Pt(2)−P(3)	105.13(9)	Pt(3)−P(3)−Pt(2)	96.58(10)
P(3)−Pt(3)−P(4)	168.48(9)				

Table 4. Selected Bond Lengths (Å) and Angles (deg) for **5**·CH_2Cl_2

Pt(1)−C(1)	2.064(5)	Pt(1)−C(7)	2.077(5)	Pt(1)−P(1)	2.2960(13)
Pt(1)−P(2)	2.3561(13)	Pt(1)−Pt(2)	2.7030(4)	Pt(2)−P(1)	2.2371(13)
Pt(2)−P(2)	2.2533(13)	Pt(2)−P(3)	2.2754(13)	Pt(2)−Pt(3)	2.7414(3)
Pt(3)−C(13)	2.075(5)	Pt(3)−P(3)	2.2262(13)	Pt(3)−P(4)	2.2402(14)
C(1)−Pt(1)−C(7)	83.85(18)	C(1)−Pt(1)−P(1)	88.35(14)	P(1)−Pt(2)−Pt(1)	54.40(3)
C(7)−Pt(1)−P(1)	167.36(13)	C(1)−Pt(1)−P(2)	165.16(14)	P(3)−Pt(2)−Pt(1)	154.05(3)
C(7)−Pt(1)−P(2)	84.41(12)	P(1)−Pt(1)−P(2)	104.71(5)	P(2)−Pt(2)−Pt(3)	97.53(3)
P(1)−Pt(2)−P(2)	110.24(5)	P(1)−Pt(2)−P(3)	100.35(5)	Pt(1)−Pt(2)−Pt(3)	152.737(10)
P(2)−Pt(2)−P(3)	149.12(5)	P(3)−Pt(3)−P(4)	106.60(5)	C(13)−Pt(3)−P(4)	94.81(14)
P(2)−Pt(2)−Pt(1)	55.88(3)	P(3)−Pt(3)−Pt(2)	53.31(3)	C(13)−Pt(3)−Pt(2)	105.13(14)
P(1)−Pt(2)−Pt(3)	151.91(4)	Pt(2)−P(1)−Pt(1)	73.20(4)	P(4)−Pt(3)−Pt(2)	158.48(3)
P(3)−Pt(2)−Pt(3)	51.67(3)	Pt(3)−P(3)−Pt(2)	75.02(4)	Pt(2)−P(2)−Pt(1)	71.77(4)
C(13)−Pt(3)−P(3)	158.43(14)				

distances and angles are listed in Table 4. Two nearly identical molecules of complex **5** are found to exist in the asymmetric part of the unit cell, and only one of these will be described here because the parameters of the other are very similar. As expected, **5** is a trinuclear complex whose main difference with respect to the structure of **3**, discussed above, is the absence of the bridging iodo ligand. This makes for a total valence electron count of 44, which implies the existence of two Pt−Pt bonds [Pt(1)−Pt(2) and Pt(2)−Pt(3) distances are 2.703(1) and 2.741(1) Å, respectively]. The disposition of the three Pt atoms is also nearly linear [Pt(1)−Pt(2)−Pt(3) = 152.7(1)°]. The "Pt(1)(μ-P)$_2$Pt(2)" fragment is planar, with more acute Pt−P−Pt angles than the analogous ones in **3** [cf. 73.2(1)° and 71.8(1)° in **5** vs 102.1(1)° and 104.4(1)° in **3**], which corresponds to diphenylphosphido ligands bridging a Pt−Pt system. This structural feature is also repeated at P(3) [cf. 75.0(1)° in **5** vs 96.6(1)° in **3**]. The core of **5** is more planar than that of **3**, with the dihedral angle between "Pt(1)P(1)P(2)Pt(2)" and "Pt(2)P(3)Pt(3)" being only 6.6(1)°. The environment of Pt(1) is essentially square planar, but those of Pt(2) and Pt(3) are more unusual. Pt(2) is surrounded by the three bridging phosphido groups, and Pt(3) is bonded to a phosphido, a pentafluorophenyl, and a $PPh_2C_6F_5$ ligand. Both metal centers also form a Pt−Pt bond. A noteworthy observation is that the Pt(3)−Pt(2)−P(2) angle, 97.5(1)°, is somewhat narrower than the Pt(3)−Pt(2)−P(1) angle, which has a value of 151.9(1)°.

A drawing of the structure of the complex ion of **7** together with the atom-labeling scheme is shown in Figure 3. Selected bond distances and angles are listed in Table 5. The three Pt atoms adopt a nearly linear arrangement [Pt(1)−Pt(2)−Pt(3) = 154.2(1)°], and the two intermetallic distances are

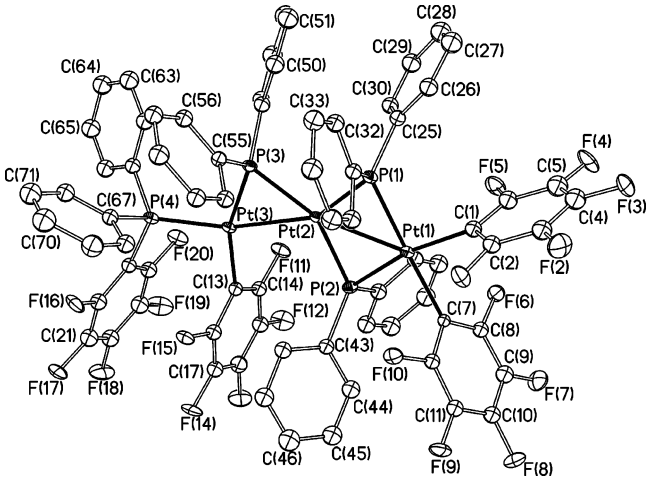

Figure 2. Molecular structure of the complex **5**·CH_2Cl_2. Ellipsoids are drawn at their 50% probability level.

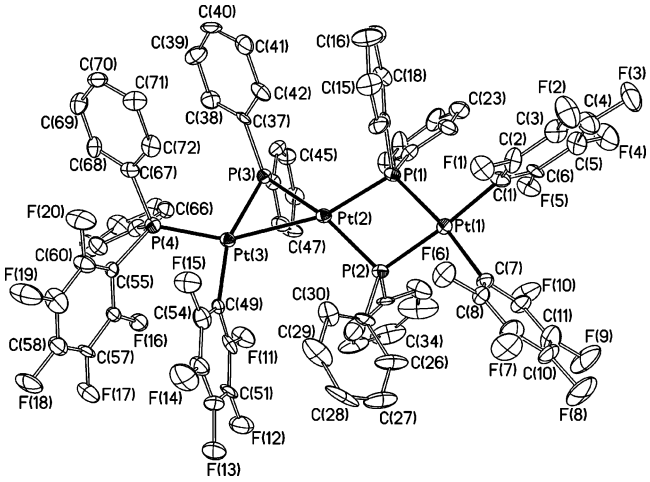

Figure 3. Molecular structure of the anion of complex **7**. Ellipsoids are drawn at their 50% probability level.

Table 5. Selected Bond Lengths (Å) and Angles (deg) for **7**

Pt(1)−C(1)	2.066(12)	Pt(1)−C(7)	2.078(12)	Pt(1)−P(2)	2.276(3)
Pt(1)−P(1)	2.306(3)	Pt(2)−P(3)	2.284(3)	Pt(2)−P(1)	2.308(3)
Pt(2)−P(2)	2.315(3)	Pt(2)−Pt(3)	2.8481(8)	Pt(3)−C(49)	2.061(12)
Pt(3)−P(4)	2.242(3)	Pt(3)−P(3)	2.297(3)	Pt(1)···Pt(2)	3.577(1)
C(1)−Pt(1)−C(7)	88.3(5)	P(4)−Pt(3)−P(3)	103.86(11)	P(3)−Pt(2)−P(2)	165.41(11)
C(7)−Pt(1)−P(2)	96.2(3)	P(4)−Pt(3)−Pt(2)	154.47(8)	P(3)−Pt(2)−Pt(3)	51.77(8)
C(7)−Pt(1)−P(1)	172.1(3)	Pt(1)−P(1)−Pt(2)	101.67(11)	P(2)−Pt(2)−Pt(3)	120.49(8)
P(3)−Pt(2)−P(1)	113.56(11)	Pt(2)−P(3)−Pt(3)	76.89(10)	C(49)−Pt(3)−P(3)	159.7(3)
P(1)−Pt(2)−P(2)	75.85(10)	C(1)−Pt(1)−P(2)	175.1(4)	C(49)−Pt(3)−Pt(2)	108.8(3)
P(1)−Pt(2)−Pt(3)	162.81(8)	C(1)−Pt(1)−P(1)	98.7(4)	P(3)−Pt(3)−Pt(2)	51.34(8)
C(49)−Pt(3)−P(4)	96.3(3)	P(2)−Pt(1)−P(1)	76.65(11)	Pt(1)−P(2)−Pt(2)	102.36(12)

perceptibly different. While the Pt(1)−Pt(2) distance is 3.577(1) Å, the Pt(2)−Pt(3) distance is only 2.848(1) Å, consistent with the presence of a Pt−Pt bond. Pt(1) and Pt(2) are bridged by two diphenylphosphido ligands, while Pt(2) and Pt(3) are bridged by a diphenylphosphido group and a hydride ligand. In agreement with the existence of the Pt(2)−Pt(3) bond, the Pt(2)−P(3)−Pt(3) angle [76.9(1)°] is more similar to the analogous one in complex **5** than that in compound **3**. Despite the fact that it was not possible to determine the position of the bridging hydride ligand (whose presence is unequivocally established by ^{1}H NMR; see below), the geometric environments of both Pt(2) and Pt(3) are consistent with the tetracoordination of the two metal centers. Thus, both environments can be described as square planar, with some distortion caused by the small size of the μ-H ligand and the presence of the Pt(2)−Pt(3) bond. The angles around Pt(2) and Pt(3) are listed in Table 4 and can be compared with the analogous ones found in complex **5** (see Table 5), for which the bridging hydride is absent.

Concluding Remarks

The synthesis of complexes **3**−**5** from **2** indicates that the dinuclear Pt^{III}−Pt^{III} fragment is not very stable and evolves through a PPh_2/C_6F_5 reductive coupling toward the formation of a trinuclear Pt^{II} complex. This reductive coupling contrasts with the behavior observed in the homologous heterotrinuclear Pt−Pd−Pt derivative, which evolves to the formation of the Pt^{II}−Pd^{II}−Pt^{II} through a PPh_2/PPh_2 coupling and the formation of a tetraphenyldiphosphine derivative. Elimination of the halide ligand in complexes **3** and **4** results in the formation of complex **5** (two Pt−Pt bonds) but not in the intramolecular oxidative addition of $PPh_2C_6F_5$ observed in the unsaturated "$(C_6F_5)_2Pt^{II}(\mu\text{-}PPh_2)Pt^{II}(C_6F_5)(PPh_2C_6F_5)^-$".

Experimental Section

General Comments. Literature methods were used to prepare the starting material $[NBu_4]_2[(C_6F_5)_2Pt(\mu\text{-}PPh_2)_2Pt(\mu\text{-}PPh_2)_2Pt(C_6F_5)_2]$.[10] C, H, and N analyses were performed, and IR and NMR spectra were measured as described elsewhere.[9]

Reaction of $[NBu_4]_2[(C_6F_5)_2Pt(\mu\text{-}PPh_2)_2Pt(\mu\text{-}PPh_2)_2Pt(C_6F_5)_2]$ (1) with I_2. To a yellow suspension of **1** (0.200 g, 0.081 mmol) in 1,2-dichloroethane (20 mL) was added a solution of I_2 (0.020 g, 0.081 mmol) in 1,2-dichloroethane (5 mL). After 1 min of stirring at room temperature, the red solution was evaporated to ca. 1 mL, $CHCl_3$ (2 mL) was added, and **2** crystallized: 0.118 g, 73% yield. In another experiment, the red solution was refluxed for 2 h. The yellow solution was evaporated to ca. 1 mL, and **3** crystallized as a yellow solid, which was filtered off and washed with cold 1,2-dichloroethane (2 × 0.5 mL): 0.111 g, 58% yield. Anal. Found (calcd for $C_{88}F_{20}H_{76}INP_4Pt_3$): C, 44.3 (44.7); H, 2.9 (3.2); N, 0.5 (0.6). IR (cm^{-1}): 1519 and 979 ($PPh_2C_6F_5$); 799, 781, and 772 (X-sensitive[45,46] C_6F_5). Λ_M = 61 Ω^{-1} cm^2 mol^{-1}. ^{19}F NMR (deuterioacetone, 293 K): δ −113.8 (2 *o*-F, J(Pt−F) = 374 Hz), −114.3 (2 *o*-F, J(Pt−F) = 314 Hz), −115.9 (2 *o*-F, J(Pt−F) = 439 Hz), −124.5 (2 *o*-F, $PPh_2C_6F_5$), −151.4 (1 *p*-F, $PPh_2C_6F_5$), −162.5 (2 *m*-F, $PPh_2C_6F_5$), −165.6 (2 *m*-F + 1 *p*-F), −166.4 (4 *m*-F), −167.1 (1 *p*-F), 167.4 (1 *p*-F).

Reaction of $[(C_6F_5)_2Pt(\mu\text{-}PPh_2)_2Pt(\mu\text{-}PPh_2)_2Pt(C_6F_5)_2]$ (2) with NBu_4Br. To a red solution of **2** (0.200 g, 0.104 mmol) in CH_2Cl_2 (30 mL) was added NBu_4Br (0.130 g, 0.401 mmol). After 3 days of stirring at room temperature, the yellow solution was evaporated to ca. 1 mL and kept in the freezer for 10 h. The yellow solid, **4**, was filtered off and washed with cold CH_2Cl_2 (2 × 0.5 mL): 0.078 g, 34% yield. Anal. Found (calcd for $BrC_{88}F_{20}H_{76}NP_4Pt_3$): C, 45.4 (45.6); H, 3.1 (3.3); N, 0.8 (0.6). IR (cm^{-1}): 1518 and 979 ($PPh_2C_6F_5$); 803, 781, and 771 (X-sensitive C_6F_5). Λ_M = 59 Ω^{-1} cm^2 mol^{-1}. ^{19}F NMR (deuterioacetone, 293 K): δ −113.8 (2 *o*-F, J(Pt−F) = 315 Hz), −114.2 (2 *o*-F, J(Pt−F) not measured), −115.4 (2 *o*-F, J(Pt−F) = 451 Hz), −124.7 (2 *o*-F, $PPh_2C_6F_5$), −151.4 (1 *p*-F, $PPh_2C_6F_5$), −162.5 (2 *m*-F, $PPh_2C_6F_5$), −165.7 (2 *m*-F + 1 *p*-F), −166.5 (4 *m*-F), −167.1 (1 *p*-F), 167.3 (1 *p*-F).

Reaction of $[NBu_4][(PPh_2C_6F_5)(C_6F_5)Pt(\mu\text{-}PPh_2)(\mu\text{-}Br)Pt(\mu\text{-}PPh_2)_2Pt(C_6F_5)_2]$ (4) with $AgClO_4$. To a yellow solution of **4** (0−250 g, 0.108 mmol) in CH_2Cl_2 (20 mL) was added $AgClO_4$ (0.073 g, 0.353 mmol). The mixture was stirred in the dark for 15 h, yielding a dark suspension, which was filtered through Celite. The orange solution was evaporated to ca. 1 mL, and $CHCl_3$ (5 mL) was added. After 5 days in the freezer, an orange solid, **5**, was filtered off and washed with cold $CHCl_3$ (3 × 0.5 mL): 0.053 g, 25% yield.

Synthesis of $[(PPh_2C_6F_5)(C_6F_5)Pt(\mu\text{-}PPh_2)Pt(\mu\text{-}PPh_2)_2Pt(C_6F_5)_2]$ (5). A red solution of **2** (0.520 g, 0.260 mmol) in 1,2-dichloroethane (30 mL) is refluxed for 40 h. The resulting orange solution was evaporated to ca. 1 mL, and $CHCl_3$ (3 mL) was added. An orange solid began to crystallize, and the mixture was kept in the freezer for 10 h. The orange solid, **5**, was filtered off and washed with cold $CHCl_3$ (3 × 0.5 mL): 0.468 g, 90% yield. Anal. Found (calcd for $C_{72}F_{20}H_{40}P_4Pt_3$): C, 43.3 (43.3); H, 2.0 (2.0). IR (cm^{-1}): 1519 and 981 ($PPh_2C_6F_5$); 793 and 782 (X-sensitive C_6F_5). ^{19}F NMR (CD_2Cl_2, 293 K): δ −113.6 (2 *o*-F, J(Pt−F) = 291 Hz), −118.5 (2 *o*-F, J(Pt−F) = 308 Hz), −119.0 (2 *o*-F, J(Pt−F) = 303 Hz), −1245.0 (2 *o*-F, $PPh_2C_6F_5$), −150.3 (1 *p*-F, $PPh_2C_6F_5$), −161.1 (2 *m*-F, $PPh_2C_6F_5$), −161.4 (2 *p*-F), −163.5 (2 *m*-F), −163.8 (1 *p*-F), 164.4 (4 *m*-F).

Reaction of 5 with NBu_4Br. To an orange solution of **5** (0.200 g, 0.100 mmol) in CH_2Cl_2 (20 mL) was added NBu_4Br (0.032 g, 0.100 mmol). After 7 h of stirring at room temperature, the yellow solution was evaporated to ca. 1.5 mL and ^{i}PrOH (10 mL) was added. The mixture was stirred for 2 h, and a yellow solid, **6**, was

filtered off and washed with ^{i}PrOH (3 × 0.5 mL): 0.170 g, 73% yield. Anal. Found (calcd for $BrC_{88}F_{20}H_{76}NP_4Pt_3$): C, 45.3 (45.6); H, 3.1 (3.3); N, 0.9 (0.6). IR (cm^{-1}): 1519 and 984 ($PPh_2C_6F_5$); 782 and 771 (X-sensitive C_6F_5). $\Lambda_M = 55\ \Omega^{-1}\ cm^2\ mol^{-1}$. ^{19}F NMR (deuterioacetone, 293 K): δ −113.6 (2 *o*-F, J(Pt−F) = 308 Hz), −114.1 (2 *o*-F, J(Pt−F) =320 Hz), −116.9 (2 *o*-F, J(Pt−F) = 242 Hz), −122.9 (2 *o*-F, $PPh_2C_6F_5$), −150.4 (1 *p*-F, $PPh_2C_6F_5$), −162.2 (2 *m*-F, $PPh_2C_6F_5$), −162.9 (1 *p*-F), −164.2 (2 *m*-F), −166.4 (2 *m*-F), −166.8 (2 *m*-F), −167.2 (1 *p*-F), −167.5 (1 *p*-F).

Reaction of $[NBu_4][(PPh_2C_6F_5)(C_6F_5)Pt(\mu\text{-}PPh_2)(\mu\text{-}Br)Pt(\mu\text{-}PPh_2)_2Pt(C_6F_5)_2]$ (6) with $AgClO_4$. To a yellow solution of **6** (0.150 g, 0.065 mmol) in CH_2Cl_2 (20 mL) was added $AgClO_4$ (0.020 g, 0.096 mmol). The mixture was stirred at room temperature and in the dark for 5 h and then filtered through Celite. The orange solution was evaporated almost to dryness, and $CHCl_3$ (4 mL) was added. After 24 h in the freezer, an orange solid, **5**, was filtered off and washed with cold $CHCl_3$ (3 × 0.5 mL): 0.050 g, 39% yield.

Reaction of 5 with NBu_4BH_4. To an orange solution of **5** (0.055 g, 0.027 mmol) in CH_2Cl_2 (10 mL) was added NBu_4BH_4 (0.015 g, 0.058 mmol) in MeOH (2 mL). After 30 min of stirring at room temperature, the yellow solution was evaporated almost to dryness and ^{i}PrOH (8 mL) was added. The mixture was stirred at room temperature for 1 h, and a yellow solid, **7**, was filtered off and washed with ^{i}PrOH (3 × 0.5 mL): 0.046 g, 75% yield. Anal. Found (calcd for $C_{88}F_{20}H_{77}NP_4Pt_3$): C, 47.1 (47.2); H, 3.2 (3.4); N, 0.8 (0.6). IR (cm^{-1}): 1520 and 981 ($PPh_2C_6F_5$); 779 and 773 (X-sensitive C_6F_5). $\Lambda_M = 55\ \Omega^{-1}\ cm^2\ mol^{-1}$. ^{1}H NMR ($CD_2Cl_2$, 293 K): δ −4.9 (1 μ-H, ^2J[P(4)−H] = 104 Hz, ^2J[P(1)−H] = 40 Hz, ^2J[P(2)−H] ≈ ^2J[P(3)−H] ≈ 9 Hz, ^1J(Pt−H) = 484 and 604 Hz). ^{19}F NMR (CD_2Cl_2, 293 K): δ −114.9 (2 *o*-F, J(Pt−F) = 368 Hz), −115.6 (2 *o*-F, J(Pt−F) not measured), −115.9 (2 *o*-F, J(Pt−F) = 299 Hz), −124.8 (2 *o*-F, $PPh_2C_6F_5$), −151.3 (1 *p*-F, $PPh_2C_6F_5$), −161.2 (2 *m*-F, $PPh_2C_6F_5$), −164.0 (1 *p*-F), −165.2 (2 *m*-F), −166.3 (4 *m*-F), −167.1 (1 *p*-F), 167.4 (1 *p*-F).

Reaction of 5 with CO. An orange solution of **5** (0.150 g, 0.075 mmol) in CH_2Cl_2 (10 mL) was stirred under CO (1 atm) for 6 h. Hexane (10 mL) was added, and the solution was evaporated to ca. 10 mL. After 1 h of stirring at room temperature, the orange solid was filtered off and washed four times with 3 mL of hexane. The yellow solution was evaporated to ca. 5 mL and kept in the freezer for 12 h. A pale yellow solid, **8**, crystallized and was filtered off and washed with 0.5 mL of cold hexane: 0.043 g, 28% yield. Anal. Found (calcd for $C_{74}F_{20}H_{40}O_2P_4Pt_3$): C, 43.3 (43.3); H, 2.0 (1.95). IR (cm^{-1}): 1519 and 982 ($PPh_2C_6F_5$); 796 and 784 (X-sensitive C_6F_5); 2094 and 2083 [ν(C≡O)]. ^{19}F NMR ($CDCl_3$, 293 K): δ −115.2 (2 *o*-F, J(Pt−F) = 335 Hz), −116.1 (2 *o*-F, J(Pt−F) = 247 Hz), −118.3 (2 *o*-F, J(Pt−F) = 291 Hz), −122.5 (2 *o*-F, $PPh_2C_6F_5$), −147.8 (1 *p*-F, $PPh_2C_6F_5$), −159.6 (2 *m*-F, $PPh_2C_6F_5$), −160.4 (1 *p*-F), −161.0 (1 *p*-F), −162.1 (1 *p*-F), −163.4 (6 *m*-F).

X-ray Structure Determinations of $3\cdot1.4Me_2CO$, $5\cdot CH_2Cl_2$, and $[NBu_4][(PPh_2C_6F_5)(C_6F_5)Pt(\mu\text{-}PPh_2)(\mu\text{-}H)Pt(\mu\text{-}PPh_2)_2Pt(C_6F_5)_2]$ (7). Crystal data and other details of the structure analyses are presented in Table 2. Single crystals were mounted on quartz fibers in a random orientation and held in place with fluorinated oil. Data collections were performed at 100 K on a Bruker Smart CCD diffractometer using graphite-monochromated Mo Kα radiation (λ = 0.710 73 Å) with a nominal crystal-to-detector distance of 6.0 cm. For each structure, a hemisphere of data was colleted based on three ω-scan runs (starting with $\omega = -28°$) at values of $\phi = 0°$, 90°, and 180° with the detector at $2\theta = 28°$. At each of these runs, frames (606, 435, and 230, respectively) were collected at 0.3° intervals and 10 s frame^{-1}. The diffraction frames were integrated using the *SAINT* package[55] and corrected for absorption with *SADABS*.[56] Lorentz and polarization corrections were applied.

The structures were solved by direct methods. All non-H atoms of the complexes were assigned anisotropic displacement parameters, except for the atoms noted below. The H atoms were constrained to idealized geometries and assigned isotropic displacement parameters equal to 1.2 times the U_{iso} values of their respective parent atoms (1.5 times for the methyl H atoms). For $3\cdot1.4Me_2CO$, three C atoms of one of the butyl fragments of the cation are disordered over two positions that were refined with 0.5 partial occupancy. These atoms were refined isotropically, and geometric restraints were applied to them. During the refinement process, acetone solvent molecules were found in the density maps. Nevertheless, these molecules were quite diffuse, and they were modeled as three moieties with partial occupancies of 0.5, 0.5, and 0.4. These molecules were refined isotropically, and geometric restraints were applied to them. Full-matrix least-squares refinement of the models against F^2 converged to final residual indices given in Table 2.

Acknowledgment. We thank the Ministerio de Ciencia y Tecnología y Fondos FEDER (Project BQU2005-08606-C02-01) for financial support. S.I. thanks the Ministerio de Ciencia y Tecnología for a FPI grant.

Supporting Information Available: Crystallographic data of $3\cdot1.4Me_2CO$, $5\cdot CH_2Cl_2$, and **7** (CIF format). This material is available free of charge via the Internet at http://pubs.acs.org.

IC0602695

(55) *SAINT*, version 5.0; Bruker Analytical X-ray Systems: Madison, WI; 1998.
(56) Sheldrick, G. M. *SADABS empirical absorption program edition*; University of Göttingen: Göttingen, Germany, 1996.
(57) Berenguer, J. R.; Chaouche, N.; Forniés, J.; Fortuño, C.; Martín, A. *New J. Chem.* **2006**, *30*, 473−478.